Geophysical Research Letters

RESEARCH LETTER
10.1029/2020GL091409

Key Points:

- We estimate the mantle heat flow in Mars's south polar region to not exceed 10 mW/m^2
- The low mantle heat flow estimate suggests the Martian mantle to be depleted in heat-producing elements
- Based on our heat flow constraints, present-day basal melting of the south polar layered deposits is highly unlikely

Supporting Information:

- Supporting Information S1

Correspondence to:
L. Ojha,
luju.ojha@rutgers.edu

Citation:
Ojha, L., Karimi, S., Buffo, J., Nerozzi, S., Holt, J. W., Smrekar, S., & Chevrier, V. (2021). Martian mantle heat flow estimate from the lack of lithospheric flexure in the south pole of Mars: Implications for planetary evolution and basal melting. *Geophysical Research Letters*, *48*, e2020GL091409. https://doi.org/10.1029/2020GL091409

Received 26 OCT 2020
Accepted 8 DEC 2020

Martian Mantle Heat Flow Estimate From the Lack of Lithospheric Flexure in the South Pole of Mars: Implications for Planetary Evolution and Basal Melting

Lujendra Ojha[1], Saman Karimi[2], Jacob Buffo[3], Stefano Nerozzi[4], John W. Holt[4,5], Sue Smrekar[6], and Vincent Chevrier[7]

[1]Department of Earth and Planetary Sciences, The State University of New Jersey, Piscataway, NJ, USA, [2]Department of Earth and Planetary Sciences, Johns Hopkins University, Baltimore, MD, USA, [3]Thayer School of Engineering, Dartmouth College, Hanover, NH, USA, [4]Lunar and Planetary Laboratory, University of Arizona, Tucson, AZ, USA, [5]Department of Geosciences, University of Arizona, Tucson, AZ, USA, [6]Jet Propulsion Laboratory, California Institute of Technology, Pasadena, California, USA, [7]Arkansas Center for Space and Planetary Sciences, University of Arkansas, Fayetteville, AR, USA

Abstract Heat flow measurements are important for our understanding of planetary interior composition, structure, and evolution. In the absence of direct measurement, a first-order estimate of a planet's interior heat flow can be made by modeling the lithosphere's viscoelastic response to stress exerted by large surface loads. Here, we model the Martian lithosphere's viscoelastic response to the south polar layered deposits and estimate the local mantle heat flow to be less than ~10 mW/m^2. Combined with our previous estimate of the low mantle heat flow from the north polar region (~7 mW/m^2), our results suggest that the Martian mantle may be globally depleted in heat-producing elements. The relatively low mantle heat flow has significant implications for Mars' long-term thermal evolution and on the possibility of basal melting in the south polar region.

Plain Language Summary The outermost layer of a planet is called the lithosphere. The lithosphere can bend due to the weight of large mountains or thick glaciers. The total amount of the bending depends on the stress imparted by topographic loads and strength or thickness of the lithosphere, which depends on the planet's interior heat. Despite the huge amount of stress exerted by the south polar cap of mars, the lithosphere underneath is remarkably flat. In this work, we model the lithospheric bending using numerical methods and provide a first-order estimate of the heat being generated in the Martian mantle. Our results suggest that the lithosphere in the southern polar region is thick and that Mars' interior is relatively cool.

1. Introduction

The long-term geological evolution of a planet is dependent on the bulk concentration of the long-lived heat-producing element (HPE; ^{238}U, ^{235}U, ^{232}Th, and ^{40}K) and their distribution between the crust and the mantle. High enrichment of HPE in the crust depletes the mantle of heat production and lowers the mantle potential temperature. In contrast, crust with lower enrichment of HPE thermally insulates the mantle increasing the mantle potential temperature (e.g., O'Neill et al., 2005). The thermal state of a planet's mantle modulates its convection, which influences volcanism, crustal tectonics, and geomagnetism (e.g., Stevenson, 2007). These geological processes directly impact hydrospheric and atmospheric processes (e.g., Halevy & Head, 2014; Kurokawa et al., 2018; Liggins et al., 2020), highlighting the importance of heat flow measurements in our understanding of the geological evolution of planets.

On Earth, surface heat flow is one of the way in which the solid interior directly interacts with the overlying cryosphere, hydrosphere, and atmosphere (e.g., Etiope & Klusman, 2002; Fahnestock et al., 2001; Mashayek et al., 2013). In various areas of the West Antarctic Ice Sheet (Fisher et al., 2015), Greenland (Bowling et al., 2019; Martos et al., 2018), and the Canadian Arctic (e.g., Rutishauser et al., 2018), subglacial lakes are formed by geothermal heat. Radiogenic heat-driven hydrothermal systems have been discovered in the Paleozoic Mt. Gee-Mt. Painter system in the Northern Flinders region of South Australia (Brugger et al., 2005, 2011). Recently, several putative subglacial lakes have been proposed to exist beneath the south

polar layered deposits (SPLD) on Mars (Lauro et al., 2020; Orosei et al., 2018). Given the low mean annual surface temperature in the south polar region of Mars (<160 K), any subglacial body of water in this region will require a substantial reduction in their eutectic temperature and/or high geothermal heat flow (e.g., Sori & Bramson, 2019). Sori and Bramson. (2019) suggested that a geothermal heat flux over 72 mW/m^2 would be needed for basal melting to occur beneath the SPLD under the most favorable compositional conditions. The feasibility of such high geothermal heat flow values in present-day Mars, however, remains unclear.

Previously, Ojha et al. (2019) used available radar constraints and finite element models to estimate the mantle heat flow in Mars' north polar region. Despite exerting more than 10 MPa of stress on the underlying lithosphere, the surface underneath the north polar cap is found to be flat (≤200 m of deflection; Phillips et al., 2008; Selvans et al., 2010). Using this radar constraint and viscoelastic modeling of the lithosphere, Ojha et al. (2019) estimated that the heat flow from the mantle in the north polar region could not exceed 7 mW/m^2. Here, we expand on that work and use similar radar constraints from the SPLD to estimate the mantle heat flow in the south polar region of Mars. We first discuss the implication of our mantle heat flow estimates on Mars' geophysical evolution. We then estimate the geothermal heat flow required for the basal melting of various briny ice at the SPLD and discuss its possibility given our heat flow constraints.

2. Methods

The apparent surface age of the south polar caps of Mars is estimated to be from 5–10 Ma (Herkenhoff & Plaut, 2000) to 30–100 Ma using crater counts (Koutnik et al., 2002). Thus, modeling the lithospheric response to these young topographic loads can provide a first-order estimate of the present-day background heat flow. Due to the lack of direct measurements, one of the most widely used techniques to estimate heat flow involves estimating the elastic thickness of the lithosphere (T_e) by using gravity and topography data (e.g., Grott & Breuer, 2008; McGovern, 2004; McGovern et al., 2002; Phillips et al., 2008). The lithosphere's elastic thickness (T_e) is the upper layer of a terrestrial planet that supports stresses over a geologically long interval and is a measure of the lithosphere resistivity to bending under the application of an applied load. Consequently, the lithospheric flexure magnitude will depend largely on the weight/wavelength of the surface load and the thickness of the lithosphere (Figure 1). The main factor that determines the elastic thickness of the lithosphere is its thermal structure (Hyndman et al., 2009); thus, it is possible to indirectly estimate the interior heat flow of a planet by modeling the observed deformation of the lithosphere in response to large topographic loads (e.g., Ojha et al., 2019). The surface heat flow of a planet (q_s) primarily includes contributions from the heat originating from radiogenic decay of HPE within the crust (q_c), the upper mantle (q_m), and the lower mantle (q_b) (Figure 1). If the stress imparted by topographic loads on a planet's surface is known, then a first-order estimate of q_b can be made by modeling the lithosphere's viscoelastic response.

2.1. Stress Imposed by the SPLD and the Lithospheric Deflection Magnitude

The south polar region of Mars contains a large volume of H_2O ice in combination with lesser amounts of CO_2 ice and dust (e.g., Bierson et al., 2016; Phillips et al., 2011). Given the SPLD's volume of 1.6×10^6 km^3 (Plaut et al., 2007) and a mean gravity-derived density of ~1,270 kg/m^3 (e.g., Li et al., 2012; Wieczorek, 2008), the mass of the SPLD is approximately 2×10^{18} kg. We used the mean gravity-derived density of ~1,270 kg/m^3 and radar-derived relief maps (e.g., Plaut et al., 2007) to estimate the stress experienced by the underlying lithosphere from the SPLD. An explicit assumption in our stress estimation is that the substrate underneath the SPLD is flat, supported by previous radar mapping of the basal interface (Plaut et al., 2007).

Similar to our previous work in the north polar region (Ojha et al., 2019), we extract stress profiles from the SPLD and fit various functions to approximate the stress profile (Text S1; Figure S1).

We equate the magnitude of surficial downwarping observed in the Mars Advanced Radar for Subsurface Ionosphere Sounding (MARSIS) radargrams to the magnitude of the lithospheric deflection in the south polar region. Although confounded by the southern highland's rugged topography, on a regional scale, the surficial downwarping underneath the SPLD does not exceed 500 m anywhere (Plaut et al., 2007). The vertical resolution of the MARSIS data is ~85 m in water ice, with an estimated uncertainty on a given

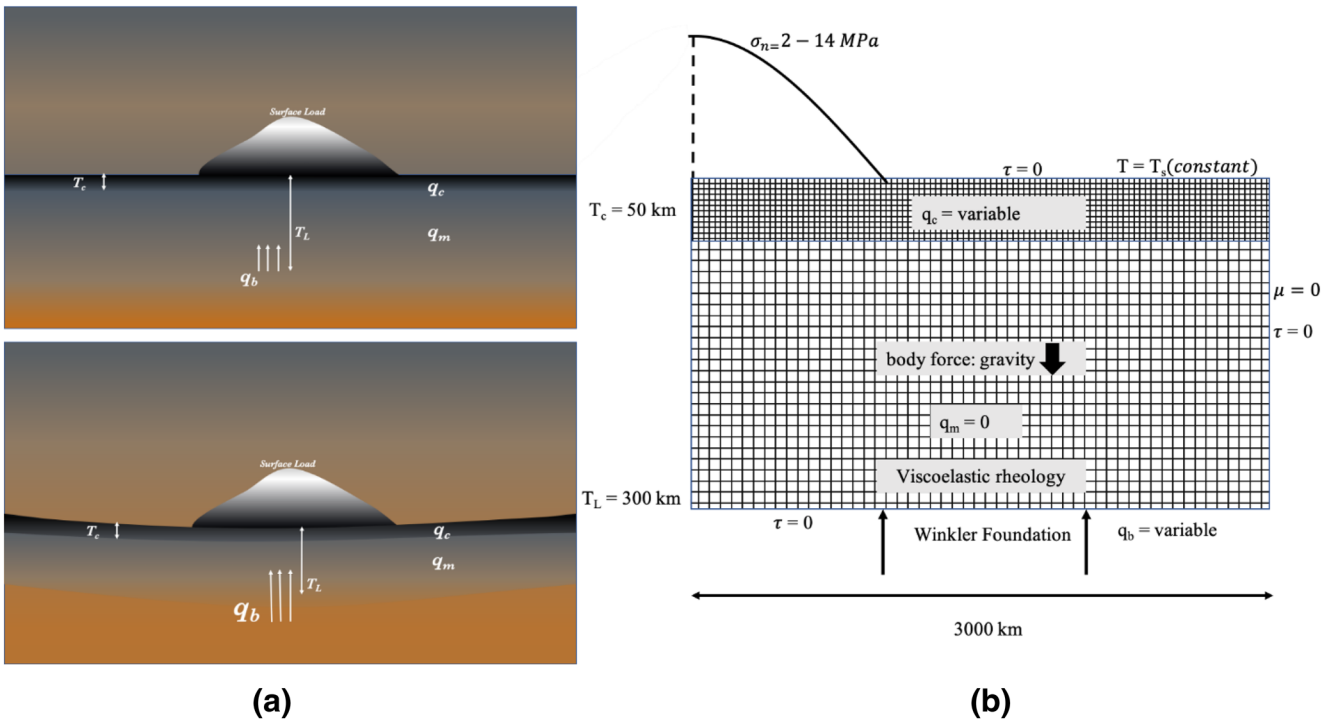

Figure 1. (a) Schematic illustrating the setup for the estimation of the mantle heat flow. The surface heat flow (q_s) includes heat generated by radiogenic decay of HPE within the crust (q_c), upper mantle (q_m), and the lower mantle (q_b). Lithospheric flexure will primarily depend on q_b. The thickness of the crust (T_c) and the lithosphere (T_L) are set to 50 and 300 km, respectively. (b) FEM mesh (axisymmetric and not to scale) used for estimating the mantle heat flow. τ, shear stress; σ_n, normal stress; μ, velocity. The σ_n profile shows the stress from SPLD as a distributed load (see Figure 2). FEM, finite element method; HPE, heat-producing element; SPLD, south polar layered deposit.

measurement less than 120 m. Plaut et al. (2007) used a dielectric constant of three to covert time delay to depth. A reasonable variation in the dielectric constant of ±0.5, would add an error of 10% in the depth estimate (Plaut et al., 2007). The presence of dust and CO_2 ice within the SPLD (e.g.,Phillips et al., 2011; Wieczorek, 2008) can further increase the uncertainty in the depth estimate. Given these uncertainties, we use an extremely conservative estimate that the maximum deflection underneath the SPLD (at the center of the topographic load) does not exceed 1 km.

2.2. Thermal and Mechanical Simulation of the Lithosphere

The viscoelastic response of the Martian lithosphere to the SPLD was modeled using the finite element package Marc-Mentat. Here, we only summarize the methodology, and interested readers are referred to several previous works (e.g., Karimi & Dombard, 2016; Karimi et al., 2016; Ojha et al., 2019) for a detailed description.

We use dual-layered, axisymmetric planar finite element mesh within which a single crustal layer overrides a mantle to mimic the Martian counterpart. Since the objective of our investigation is to match the observed surface downwarping in MARSIS radargrams, the mesh has depth-dependent resolution such that the crust has more elements per unit area than the mantle. In total, the mesh has 10^4 elements. The wavelength of the SPLD is relatively small (<10°; Figure S1), so the flexural response of the lithosphere can be sufficiently modeled in a planar mesh. We set the depth and the width of the mesh to be 350 and 3,000 km wide so that the far edge boundaries do not notably impact the model results. We use the gravity derived crustal thickness estimate of ~60 km for the southern highlands in our model (e.g., Neumann et al., 2004). The enrichment of the HPE in the crust can significantly affect the geothermal gradient and is a parameter that we explore in our models.

A steady-state thermal simulation is run on the mesh by setting the following boundary conditions. We set the surface temperature at the base of the SPLD (i.e., top of the Martian crust) to be 165 K (Piqueux et al., 2008). As discussed below, plausible variations in this temperature value have a negligible impact on the lithospheric deflection magnitude. We assume the crust and mantle density to be 2,900 and 3,500 kg/m^3, respectively, similar to numerous previous works (e.g., McGovern et al., 2004; Neumann et al., 2004; Zuber et al., 2000). The mantle and crustal thermal conductivities are set to 4 and 2.5 W/m·K, respectively (Schumacher & Breuer, 2006). The elastic Young's moduli for the crust and mantle are set to 60 and 120 GPa, respectively, while the Poisson's ratio for both is set to 0.25 (Turcotte & Schubert, 2014). We do, however, vary both thermal conductivity and Young's modulus to assess their effect on our final results. We set the heat flow from the domain's left and right boundaries to zero and vary the mantle heat flow (Figure 1). The outputs from the thermal simulation are used to drive the mechanical simulation. The mechanical simulation runs for a maximum of 10 million years, sufficient to model over 90% of the lithospheric deformation (Ojha et al., 2019). The composition of the crust and mantle is uniform with depth, and their viscoelastic rheology is temperature-dependent (e.g., Caristan, 1982; Karato & Wu, 1993; Mackwell et al., 1998).

2.3. Thermophysical Evolution of the SPLD

To simulate the thermophysical evolution of the SPLD subject to variable basal heat flux, we simplified the three-phase ice sheet deposition and densification model of Ojha et al. (2020). This model simulates the deposition, densification, and thermophysical evolution of Martian ice sheets, including the production of basal melt by implementing an implicit finite difference method to solve the volume-averaged thermal conductivity equation in the ice sheet alongside the enthalpy method to calculate basal melt volumes. More details about this model is provided in Text S2.

3. Results and Discussion

We find that the SPLD imparts up to 14 MPa of normal stress on the underlying lithosphere (Figure S1). The slight underestimation of the observed stress profile by our linear approximation does not notably impact the results since the goal here is to provide an upper limit on q_b. We first disregard the heat flow contribution from both the crust and lithospheric mantle and only vary the heat flow provided by the lower mantle to the lithosphere (q_b; Figure 1). Both the crust and the lithospheric mantle can be significant heat sources, so our simplification is clearly an idealized scenario. However, by disregarding both q_c and q_m, we can place an upper limit on q_b. Assuming hydrous rheology for the crust and the mantle, we find that q_b higher than 10 mW/m^2 produce lithospheric deflection over 1 km at the center of the SPLD (Figure 2). Even at a distance of ~500 km from the center of the SPLD, the lithospheric deflection should exceed 500 m for q_b larger than 10 mW/m^2 (Figure 2). There is no evidence for regional surface downwarping exceeding 500 m in MARSIS radargrams of the SPLD at this distance (see Figures 1 and 2 of Plaut et al., 2007). Thus, we find 10 mW/m^2 to be a conservative upper limit on q_b.

Having established 10 mW/m^2 as a preliminary estimate of q_b in the south polar region of Mars, we explore how various parameters involved in our finite element models can affect this estimate. While the Martian crust can be a large source of heat (e.g., Hahn et al., 2011), the inclusion of q_c will only act to increase the magnitude of the lithospheric deflection, so it does not change the upper limit estimate of q_b (Figure 2). We use a crustal density of 2,900 kg/m^3, but recent gravity work suggests that the crustal density of Mars could be as low as 2,500 kg/m^3 (Goossens et al., 2017). We tested our model's sensitivity to variation in crustal density but found it to have a negligible effect on the lithospheric flexure. However, if the lower density of the Martian crust is due to impact-induced fractures, then resulting variations in thermal conductivity could notably affect our heat flow estimates. The thermal conductivity (k_c) of the Martian crust is likely depth-dependent, largely modulated by variations in temperature and pressure (Schumacher & Breuer, 2006). The k_c of terrestrial crustal rocks is observed to vary between 1 and 4 W/m·K (Majorowicz et al., 2019), and a similar range is expected for the Martian crust (Schumacher & Breuer, 2006). Here, we varied the k_c of the crust between 2.5 and 4 W/m·K and find that they do not affect our upper limit on q_b (Figure 2). For a q_b of 10 mW/m^2, the magnitude of the lithospheric deflection is slightly higher than 1 km at the center when

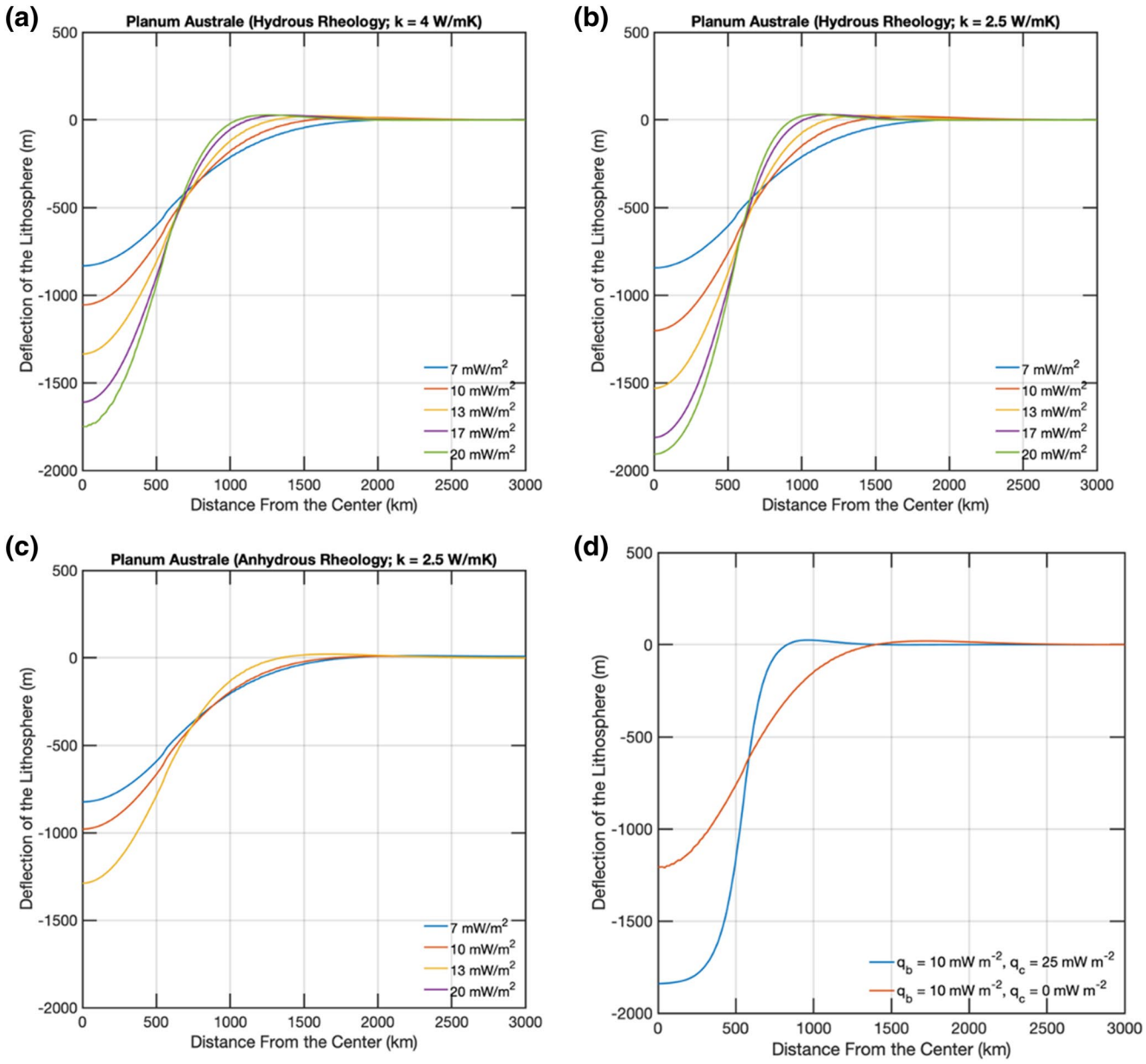

Figure 2. Flexure models of the Martian lithosphere for various thermal conditions. (a) The modeled deflection of the lithosphere from the weight of Planum Australe for various q_b and assuming k_c of 4 W/m·K and hydrous rheology. (b) Same as (a), but assuming k_c of 2.5 W/m·K. (c) Same as (b) but assuming anhydrous rheology. (d) The modeled deflection of the lithosphere showing the influence of crustal heat sources. All other parameters are identical among the four models (see Table S1 for a detailed summary of the parameters).

k_c is assumed to be 4 W/m·K. The lithospheric deflection magnitude increases when a lower k_c value of 2.5 W/m·K is assumed, which is expected as lower conductivity leads to a higher degree of thermal insulation. If the bulk average thermal conductivity of the Martian crust is even lower than 2.5 W/m·K, then our upper limit of q_b is likely an overestimate. In summary, the end member scenarios presented in Figure 2 illustrate that regardless of our choice of k_c, the lithospheric deflection should exceed 1 km at the center of the SPLD for q_b greater than 10 mW/m^2. The lithospheric deflection magnitude is smaller in anhydrous rheology (Figure 2). However, even if the Martian interior is assumed to be anhydrous, the magnitude of the lithospheric deflection should exceed 1 km at the center of the SPLD for q_b higher than 10 mW/m^2 (Figure 2). We also varied the Young's modulus of the Martian crust but reasonable variations are not found

to impact our upper limit on q_b (Text S3). In summary, reasonable variations in the rheology and thermal parameters do not change our upper limit estimate of q_b.

The lithospheric deflection in the south polar region may be small if insufficient time has passed since the emplacement of the SPLD for viscoelastic response to reach an equilibrium. Previously, we have shown that the majority of flexure occurs within 100,000 years of emplacement of the load (Ojha et al., 2019). Crater counting studies suggest the emplacement age of the SPLD to be 10–100 Ma (Herkenhoff & Plaut, 2000; Koutnik et al., 2002) and we run our models for 10 Ma; therefore, we can preclude ongoing or recent flexure development as a potential source of the estimated low q_b. We also sought to understand if variations in surface temperature could impact our flexure simulation. Mars' obliquity evolves over long timescales due to secular orbital perturbations (e.g., Laskar et al., 2004). The variation in obliquity leads to heterogeneity in the mean surface temperature over geological timescales. The thermal time constant for a >300 km lithosphere (as considered here) is 10^9 years which is substantially longer than the time scale of our simulation. Thus, variation in surface temperature should not change our q_b upper limit. We previously varied the surface temperature by ±20 K in the north polar region and observed no major change in the magnitude of the lithospheric deflection (Ojha et al., 2019).

Our estimate of q_b could change if radar observations have either underestimated or overestimated the actual extent of the surface bending in the south polar regions of Mars. There is no evidence of significant basal deflection in the north polar region (Brothers et al., 2015; Grima et al., 2009; Nerozzi & Holt, 2019; Phillips et al., 2008; Putzig et al., 2009; Selvans et al., 2010) or the south polar region of Mars (Abu Hashmeh et al., 2020; Plaut et al., 2007). Recently, Broquet et al. (2020) modeled the deflection of the north polar region of Mars by assuming the integrated permittivity of the north polar layered deposits (NPLD) and basal unit to be 2.75 (+0.40, −0.35) and estimated a maximum absolute deflection of 400 m at the center of the polar cap and 250 m below Gemina Lingula. Using these estimates of deflection, the authors derived a heat flow of 13–20 mW/m^2 at the north polar region (Broquet et al., 2020), which is higher than the estimate provided in Ojha et al. (2019). However, depth correction for the radar assuming permittivity less than 3.15 creates short-wavelength topography at the base that mimics the surface topography of the NPLD (i.e., mirror image; Figure S3). This is neither geophysically nor geologically plausible since there should be no correlation between topography in the upper NPLD, a relatively recent geologic feature undergoing modification, and the base of Planum Boreum (PB). Statistical treatment of this concept is given by Grima et al. (2009), who derived a dielectric constant of 3.10 ± 0.12 using 140,000 SHARAD data points.

Furthermore, an integrated permittivity of less than three implies a large fraction (> at least 10%) of the north polar cap to have CO_2 composition. The vast majority of NPLD layers are laterally continuous for 100s of km and are exposed in visible outcrops along spiral troughs and steep scarps all around PB (Becerra et al., 2016; Fishbaugh et al., 2010; Nerozzi & Holt, 2018; Tanaka et al., 2008). The yearly CO_2 ice balance is negative at the north pole, and any exposed CO_2 ice should sublimate during northern spring and summer (e.g., Blackburn et al., 2010). Similarly, CO_2 clathrate hydrates are unstable under present conditions during all seasons, except perhaps under ideal conditions in northern winter (Herri & Chassefière, 2012). Yet, there is no documented evidence of the presence or sublimation of CO_2 ice or clathrate hydrates within NPLD and basal unit layers. Recent atmospheric modeling results also suggest that substantial CO_2-ice cannot accumulate in the north polar cap (Buhler et al., 2020).

Similar to the north polar region, the basal surface in the SPLD is found to be remarkably flat over 100s of km (Plaut et al., 2007). A more recent mapping of the SPLD basal interface also finds the SPLD subsurface to be regionally flat (Abu Hashmeh et al., 2020). The surficial downwarping underneath the SPLD is likely less than our conservative estimate of 1 km (e.g., Plaut et al., 2007). If surficial downwarping is ∼500 m, the mantle heat flow may be lower than 7 mW/m^2, similar to our estimate of mantle heat flow in the north polar region (Ojha et al., 2019). Thus, reasonable variations in radar mapping of the basal surface do not notably change our upper limit on q_b at the south polar region.

Given their incompatible nature, a strong fractionation of HPE in the Martian crust is an inevitable consequence of mantle magmatism. The degree of HPE fractionation depends on the crustal thickness. Previously, Spohn (1991) suggested the Martian southern highlands' formation depleted the mantle of ∼50% of the HPE and lowered Mars' internal temperature by ∼200 K (Spohn, 1991). Taylor et al. (2006) modeled that

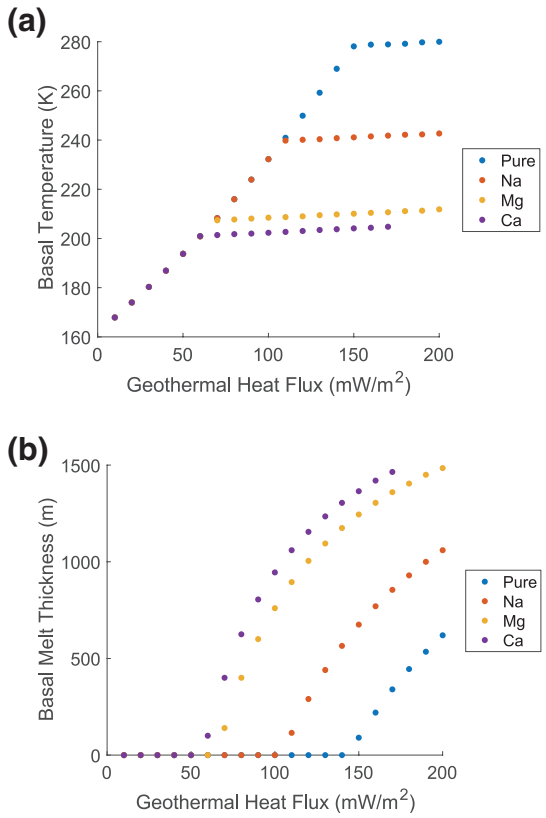

Figure 3. Thermophysical evolution of the ice sheet at the south polar region of Mars. (a) The basal temperature at the base of the SPLD as a function of geothermal heat flux for various perchlorates. Once the eutectic temperature of the salt-ice mixture is achieved, the temperature remains constant. (b) Basal melt thickness (per m^2 column of ice) as a function of geothermal heat for a variety of perchlorate species. SPLD, south polar layered deposit.

50% of the bulk Martian Th is in the crust for a nominal crustal thickness of 57 km. If the thickness of the crust is 81 km, then Th in excess of 70% may be present in the Martian crust. Numerical modeling by Plesa et al (2018) also suggest a strong fractionation (>67%) of HPE in the Martian crust. On Earth, HPE are replenished in the mantle via subduction of the crust, however, on a single-lid planet like Mars, the mantle would have been depleted by the formation of a mafic protocrust and subsequent volcanism (e.g., Hamilton, 2019).

Evidence for the depletion of HPE in the Martian mantle can be found in the chemical analyses of Martian meteorites. A basaltic shergottite called QUE 94201 is known to be significantly depleted in the concentration of HPE (Jones, 2003). The source region of the QUE is depleted in HPE comparted to the upper mantle of the Earth by a factor of 6, and the heat production rate from the QUE source regions is lower by an order of magnitude compared to the heat production rate that can be expected from a chondritic source (Jones, 2003). The low inferred mantle heat flow estimates in the north and the south polar region of Mars from our work are thus entirely consistent with the notion of a HPE-enriched Martian crust with a depleted mantle.

A major thermal implication of our result is that a strong crustal fractionation of HPE would deplete the heat production in the mantle and lower the mantle temperature, leading to a decrease in melt production over time (O'Neill et al., 2005). Thus, as observed, over time volcanism would be expected to wane on Mars. Recent analyses of radar data from the MARSIS has interpreted bright subsurface reflectors as indications of liquid water at the base of the SPLD (Lauro et al., 2020; Orosei et al., 2018). Augmentation of the background heat flux by at least 72 mW/m^2 provided by extremely recent magmatism has been proposed as a potential source of heat for the putative liquid water (Sori & Bramson, 2019). We revisit this problem with our thermal model and find that the minimal geothermal heat flow needed to produce melt is ~60 mW/m^2 for Ca perchlorate enriched basal melt (Figure 3). This is in good agreement with the 72 mW/m^2 predicted by Sori and Bramson (2019). Our estimation is slightly lower because our surficial frost layer is 5-m thick as opposed to the 1-m thick frost layer implemented by Sori and Bramson (2019), leading to enhanced insulation and a lower required geothermal heat flux to induce basal melting (Figure 3).

The surface heat flow in the south polar region of Mars, including an average crustal heat flow of 10 mW/m^2 (Hahn et al., 2011) and a mantle heat flow of 10 mW/m^2 as estimated here, is nowhere enough to induce any melting. Liquid water in the south polar region would therefore require elevated heat flow, perhaps due to recent volcanism (e.g., Sori & Bramson, 2019). Sori and Bramson (2019) considered the elevated heat flow due to a small (~5 km) magmatic intrusion. We ran several flexure models that included heat from a recent magmatic intrusion but found it to not affect the lithospheric flexure (Text S4; Figure S4). Thus, we can neither confirm nor reject whether such intrusion is present or even possible in present-day Mars. If the Martian mantle is globally depleted in HPE, then recent volcanism is likely rare. A possible scenario for the Martian interior is that it consists of a more enriched nakhlite source region, that is insulated by the more depleted shergottite mantle, and an enriched crust (Jones, 2003). An occasional mantle plume from the nakhlite source region could allow recent volcanism to occur on Mars (Neukum et al., 2004; Sori & Bramson, 2019), while the depleted shergottite mantle and the enriched crust helps explain the lack of significant flexure in the polar region.

Lauro et al. (2020) considered the recent magmatic activity as a solution to be largely speculative and instead provided an alternative solution whereby the putative subglacial water bodies result from the "known physical and chemical properties of aqueous solutions." Namely, the authors suggest the subglacial water

bodies to be due to supercooled Mg-and-Ca perchlorate-H_2O solutions. Laboratory work has demonstrated that supercooled perchlorate-H_2O solutions can remain in liquid form down to 150 K (Toner et al., 2014). However, the supercooled state of Mg-and-Ca perchlorates is inherently metastable and not stable over geologic time scales (Toner et al., 2014). Furthermore, other studies suggest that salt solutions resemble an amorphous glass phase at this temperature rather than a liquid (Chevrier & Altheide, 2008). The other issue with this formation mechanism in the SPLD is the sheer volume of Ca-and-Mg perchlorates required to explain the putative body of water. Lauro et al. (2020) estimate that the main body of putative water in the SPLD has a dimension of approximately 20 × 30 km. Assuming a shallow body with a thickness of 5 m, the water volume in this putative lake would equal 3×10^9 m^3. The minimum molal concentration of salt required for supercooled brine is 3.4 m for Mg-perchlorate and 4 m for Ca-perchlorate. Thus, the volume of salts required to explain the concentrated brine in the SPLD exceeds 1.4×10^9 m^3 for Mg-perchlorate and 1.8×10^9 m^3 for Ca-perchlorate. If an average density of 1,600 kg/m^3 is assumed, these volumes imply salt masses in excess of 10^{12} kg. On Earth, Na, K, and Cl bearing salts can be leached from local rocks and may be concentrated locally. However, salts like perchlorates on Mars are not derived locally but globally from the atmospheric oxidation of HCl at low surface concentration (Catling et al., 2010; Wilson et al., 2016). The process responsible for such a large sequestration of perchlorates required to explain the putative body of water in the SPLD is unknown. Alternatively, if the radar-bright regions are instead a thin layer of saline fluid or brine saturated sediments, then the volume of salt required to explain the detections would be considerably less.

4. Conclusion

The Martian lithosphere's viscoelastic response to stress exerted by the SPLD is modeled using a finite element model. Our results suggest that the heat flow provided by the mantle to the base of the lithosphere does not exceed 10 mW/m^2 in the south polar region of Mars. Along with our previous estimate of low mantle heat flow from the north polar region (Ojha et al., 2019), the lack of lithospheric flexure in the SPLD suggest that the Martian mantle may be globally depleted in HPE. We suggest a strong fractionation of HPE in the Martian crust as the most likely reason for the inferred low mantle heat flow. Basal melting of SPLD, if it is happening, requires recent magmatic intrusion events which are not easy to reconcile with the inferred thick lithosphere at the south polar region of Mars. The planned measurement of surface heat flow by Heat Flow and Physical Properties Probe (HP^3) onboard NASA's Interior Exploration using Seismic Investigations (InSight) will be critical to better understand the reasons behind the lack of lithospheric flexure in the polar regions of Mars.

Data Availability Statement

The radar data used in this work may be obtained from NASA PDS website at https://pds-geosciences.wustl.edu/missions/mro/sharad.htm. The flexure profiles may be obtained from the corresponding author.

Acknowledgments
The authors are grateful to Dr. Steven Hauck II for his assistance with the computational facilities. The authors also thank Michael Sori and an anonymous reviewer whose comments helped improve and clarify this manuscript.

References

Abu Hashmeh, N. A., Whitten, J. L., & Campbell, B. A. (2020). Areal extent of subsurface basal reflectors within the south polar layered deposits. *Seventh Mars Polar Science Conference LPICo 2099*, 6047.

Becerra, P., Byrne, S., Sori, M. M., Sutton, S., & Herkenhoff, K. E. (2016). Stratigraphy of the north polar layered deposits of Mars from high-resolution topography. *Journal of Geophysical Research: Planets*, *121*(8), 1445–1471. https://doi.org/10.1002/2015JE004992

Bierson, C. J., Phillips, R. J., Smith, I. B., Wood, S. E., Putzig, N. E., Nunes, D., & Byrne, S. (2016). Stratigraphy and evolution of the buried CO_2 deposit in the Martian south polar cap. *Geophysical Research Letters*, *43*, 4172–4179. https://doi.org/10.1002/2016GL068457

Blackburn, D. G., Bryson, K. L., Chevrier, V. F., Roe, L. A., & White, K. F. (2010). Sublimation kinetics of CO_2 ice on Mars. *Planetary and Space Science*, *58*(5), 780–791. https://doi.org/10.1016/j.pss.2009.12.004

Bowling, J. S., Livingstone, S. J., Sole, A. J., & Chu, W. (2019). Distribution and dynamics of Greenland subglacial lakes. *Nature Communications*, *10*, 2810. https://doi.org/10.1038/s41467-019-10821-w

Broquet, A., Wieczorek, M. A., & Fa, W. (2020). Flexure of the lithosphere beneath the north polar cap of Mars: Implications for ice composition and heat flow. *Geophysical Research Letters*, *47*, e2019GL086746.

Brothers, T. C., Holt, J. W., & Spiga, A. (2015). Planum Boreum basal unit topography, Mars: Irregularities and insights from SHARAD. *Journal of Geophysical Research: Planets*, *120*, 1357–1375. https://doi.org/10.1002/2015JE004830

Brugger, J., Long, N., McPhail, D. C., & Plimer, I. (2005). An active amagmatic hydrothermal system: The Paralana hot springs, Northern Flinders Ranges, South Australia. *Chemical Geology*. *222*, 35–64. https://doi.org/10.1016/j.chemgeo.2005.06.007

Brugger, J., Wülser, P.-A., & Foden, J. (2011). Genesis and preservation of a uranium-rich Paleozoic epithermal system with a surface expression (Northern Flinders Ranges, South Australia): Radiogenic heat driving regional hydrothermal circulation over geological timescales. *Astrobiology*, *11*, 499–508.

Buhler, P. B., Ingersoll, A. P., Piqueux, S., Ehlmann, B. L., & Hayne, P. O. (2020). Coevolution of Mars's atmosphere and massive south polar CO_2 ice deposit. *Nature Astronomy*. *4*, 364–371. https://doi.org/10.1038/s41550-019-0976-8

Caristan, Y. (1982). The transition from high temperature creep to fracture in Maryland diabase. *Journal of Geophysical Research*, *87*(B8), 6781–6790. https://doi.org/10.1029/JB087iB08p06781

Catling, D. C., Claire, M. W., Zahnle, K. J., Quinn, R. C., Clark, B. C., Hecht, M. H., & Kounaves, S. (2010). Atmospheric origins of perchlorate on Mars and in the Atacama. *Journal of Geophysical Research*, *115*, E00E11. https://doi.org/10.1029/2009je003425

Chevrier, V. F., & Altheide, T. S. (2008). Low temperature aqueous ferric sulphate solutions on the surface of Mars. *Geophysical Research Letters*, *35*(22). https://doi.org/10.1029/2008GL035489

Etiope, G., & Klusman, R. W. (2002). Geologic emissions of methane to the atmosphere. *Chemosphere*, *49*(8), 777–789. https://doi.org/10.1016/S0045-6535(02)00380-6

Fahnestock, M., Abdalati, W., Joughin, I., Brozena, J., & Gogineni, P. (2001). High geothermal heat flow, basal melt, and the origin of rapid ice flow in central Greenland. *Science*, *294*(5550), 2338–2342. https://doi.org/10.1126/science.1065370

Fishbaugh, K. E., Byrne, S., Herkenhoff, K. E., Kirk, R. L., Fortezzo, C., Russell, P. S., & McEwen, A. (2010). Evaluating the meaning of "layer" in the martian north polar layered deposits and the impact on the climate connection. *Icarus*, *205*(1), 269–282. https://doi.org/10.1016/j.icarus.2009.04.011

Fisher, A. T., Mankoff, K. D., Tulaczyk, S. M., Tyler, S. W., & Foley, N. (2015). High geothermal heat flux measured below the West Antarctic Ice Sheet. *Science Advances*, *1*(6), e1500093. https://doi.org/10.1126/sciadv.1500093

Goossens, S., Sabaka, T. J., Genova, A., Mazarico, E., Nicholas, J. B., & Neumann, G. A. (2017). Evidence for a low bulk crustal density for Mars from gravity and topography. *Geophysical Research Letters*, *44*, 7686–7694. https://doi.org/10.1002/2017GL074172

Grima, C., Kofman, W., Mouginot, J., Phillips, R. J., Hérique, A., Biccari, D., et al. (2009). North polar deposits of Mars: Extreme purity of the water ice. *Geophysical Research Letters*, *36*, L03203. https://doi.org/10.1029/2008GL036326

Grott, M., & Breuer, D. (2008). The evolution of the martian elastic lithosphere and implications for crustal and mantle rheology. *Icarus*, *193*, 503–515. https://doi.org/10.1016/j.icarus.2007.08.015

Hahn, B. C., McLennan, S. M., & Klein, E. C. (2011). Martian surface heat production and crustal heat flow from Mars Odyssey Gamma-Ray spectrometry. *Geophysical Research Letters*, *38*, L14203. https://doi.org/10.1029/2011GL047435

Halevy, I., & Head, J. W. (2014). Episodic warming of early Mars by punctuated volcanism. *Nature Geoscience*, *7*, 865–868. https://doi.org/10.1038/ngeo2293

Hamilton, W. B. (2019). Toward a myth-free geodynamic history of Earth and its neighbors. *Earth-Science Reviews*, *198*, 102905. https://doi.org/10.1016/j.earscirev.2019.102905

Herkenhoff, K. E., & Plaut, J. J. (2000). Surface ages and resurfacing rates of the polar layered deposits on Mars. *Icarus*, *144*, 243–253. https://doi.org/10.1006/icar.1999.6287

Herri, J. M., & Chassefière, E. (2012). Carbon dioxide, argon, nitrogen and methane clathrate hydrates: Thermodynamic modeling, investigation of their stability in Martian atmospheric conditions and variability of methane trapping. *Planetary and Space Science*, *73*(1), 376–386. https://doi.org/10.1016/j.pss.2012.07.028

Hyndman, R. D., Currie, C. A., Mazzotti, S., & Frederiksen, A. (2009). Temperature control of continental lithosphere elastic thickness, Te vs Vs. *Earth and Planetary Science Letter*, *277*, 539–548. https://doi.org/10.1016/j.epsl.2008.11.023

Jones, J. H. (2003). Constraints on the structure of the martian interior determined from the chemical and isotopic systematics of SNC meteorites. *Meteoritics & Planetary Sciences*, *38*, 1807–1814. https://doi.org/10.1111/j.1945-5100.2003.tb00016.x

Karato, S. I., & Wu, P. (1993). Rheology of the upper mantle: A synthesis. *Science*, *260*(5109), 771–778. https://doi.org/10.1126/science.260.5109.771

Karimi, S., & Dombard, A. J. (2016). On the possibility of viscoelastic deformation of the large south polar craters and true polar wander on the asteroid Vesta. *Journal of Geophysics Research: Planets*, *121*, 1786–1797. https://doi.org/10.1002/2016JE005064

Karimi, S., Dombard, A. J., Buczkowski, D. L., Robbins, S. J., & Williams, R. M. (2016). Using the viscoelastic relaxation of large impact craters to study the thermal history of Mars. *Icarus*, *272*, 102–113. https://doi.org/10.1016/j.icarus.2016.02.037

Koutnik, M., Byrne, S., & Murray, B. (2002). South polar layered deposits of Mars: The cratering record. *Journal of Geophysical Research*, *107*, 10–11. https://doi.org/10.1029/2001JE001805

Kurokawa, H., Foriel, J., Laneuville, M., Houser, C., & Usui, T. (2018). Subduction and atmospheric escape of Earth's seawater constrained by hydrogen isotopes. *Earth and Planetary Science Letters*, *497*(1), 149–160. https://doi.org/10.1016/j.epsl.2018.06.016

Laskar, J., Correia, A. C. M., Gastineau, M., Joutel, F., Levrard, B., & Robutel, P. (2004). Long term evolution and chaotic diffusion of the insolation quantities of Mars. *Icarus*, *170*(2), 343–364. https://doi.org/10.1016/j.icarus.2004.04.005

Lauro, S. E., Pettinelli, E., Caprarelli, G., Guallini, L., Rossi, A. P., Mattei, E., et al. (2020). Multiple subglacial water bodies below the south pole of Mars unveiled by new MARSIS data. *Nature Astronomy*. https://doi.org/10.1038/s41550-020-1200-6

Li, J., Andrews-Hanna, J. C., Sun, Y., Phillips, R. J., Plaut, J. J., & Zuber, M. T. (2012). Density variations within the south polar layered deposits of Mars. *Journal of Geophysical Research*, *117*(E4). https://doi.org/10.1029/2011JE003937

Liggins, P., Shorttle, O., & Rimmer, P. B. (2020). Can volcanism build hydrogen-rich early atmospheres? *Earth and Planetary Science Letters*, *550*, 116546.

Mackwell, S. J., Zimmerman, M. E., & Kohlstedt, D. L. (1998). High-temperature deformation of dry diabase with application to tectonics on Venus. *Journal of Geophysical Research*, *103*, 975–984. https://doi.org/10.1029/97JB02671

Majorowicz, J., Polkowski, M., & Grad, M. (2019). Thermal properties of the crust and the lithosphere–asthenosphere boundary in the area of Poland from the heat flow variability and seismic data. *International Journal of Earth Sciences*, *108*, 649–672. https://doi.org/10.1007/s00531-018-01673-8

Martos, Y. M., Jordan, T. A., Catalán, M., Jordan, T. M., Bamber, J. L., & Vaughan, D. G. (2018). Geothermal heat flux reveals the iceland hotspot track underneath Greenland. *Geophysical Research Letters*, *45*(6), 8214–8222. https://doi.org/10.1029/2018GL078289

Mashayek, A., Ferrari, R., Vettoretti, G., & Peltier, W. R. (2013). The role of the geothermal heat flux in driving the abyssal ocean circulation. *Geophysical Research Letters*, *40*(12), 3144–3149. https://doi.org/10.1002/grl.50640

McGovern, P. J. (2004). Correction to "Localized gravity/topography admittance and correlation spectra on Mars: Implications for regional and global evolution. *Journal of Geophysical Research*, *109*, E07007. https://doi.org/10.1029/2004JE002286

McGovern, P. J., Solomon, S. C., Smith, D. E., Zuber, M. T., Simons, M., Wieczorek, M. A., et al. (2002). Localized gravity/topography admittance and correlation spectra on Mars: Implications for regional and global evolution. *Journal of Geophysical Research*, *107*, 5136. https://doi.org/10.1029/2002JE001854

McGovern, P. J., Solomon, S. C., Smith, D. E., Zuber, M. T., Simons, M., Wieczorek, M. A., et al. (2004). Correction to "Localized gravity/topography admittance and correlation spectra on {M}ars: Implications for regional and global evolution". *Journal of Geophysical Research*, *109*, E07007. https://doi.org/10.1029/2004JE002286

Nerozzi, S., & Holt, W. J. (2018). Earliest accumulation history of the north polar layered deposits, Mars from SHARAD. *Icarus*, *308*, 128–137. https://doi.org/10.1016/j.icarus.2017.05.027

Nerozzi, S., & Holt, J. W. (2019). Buried ice and sand caps at the north pole of Mars: Revealing a record of climate change in the cavi unit with SHARAD. *Geophysical Research Letters*, *46*(13), 7278–7286. https://doi.org/10.1029/2019GL082114

Neukum, G., Jaumann, R., Hoffmann, H., Hauber, E., Head, J. W., Basilevsky, A. T., et al. (2004). Recent and episodic volcanic and glacial activity on Mars revealed by the High Resolution Stereo Camera. *Nature*, *432*, 971–979. https://doi.org/10.1038/nature03231

Neumann, G. A., Zuber, M. T., Wieczorek, M. A., McGovern, P. J., Lemoine, F. G., & Smith, D. E. (2004). Crustal structure of Mars from gravity and topography. *Journal of Geophysical Research*, *109*(E8). https://doi.org/10.1029/2004JE002262

Ojha, L., Buffo, J., Karunatillake, S., & Siegler, M. (2020). Groundwater production from geothermal heating on early Mars and implication for early martian habitability. *Science Advances*, *6*(49), eabb1669. https://doi.org/10.1126/sciadv.abb1669

Ojha, L., Karimi, S., Lewis, K. W., Smrekar, S. E., & Siegler, M. (2019). Depletion of heat producing elements in the Martian mantle. *Geophysical Research Letters*, *46*(22), 12756–12763. https://doi.org/10.1029/2019GL085234

Orosei, R., Lauro, S. E., Pettinelli, E., Cicchetti, A., Coradini, M., Cosciotti, B., et al. (2018). Radar evidence of subglacial liquid water on Mars. *Science*, *361*(6401), 490–493. https://doi.org/10.1126/science.aar7268

O'Neill, C., Moresi, L., & Lenardic, A. (2005). Insulation and depletion due to thickened crust: Effects on melt production on Mars and Earth. *Geophysical Research Letters*, *32*(14). https://doi.org/10.1029/2005GL022855

Phillips, R. J., Davis, B. J., Tanaka, K. L., Byrne, S., Mellon, M. T., Putzig, N. E., et al. (2011). Massive CO_2 ice deposits sequestered in the south polar layered deposits of Mars. *Science*, *332*, 838–841.

Phillips, R. J., Zuber, M. T., Smrekar, S. E., Mellon, M. T., Head, J. W., Tanaka, K. L., et al. (2008). Mars north polar deposits: Stratigraphy, age, and geodynamical response. *Science*, *320*, 1182–1185. https://doi.org/10.1126/science.1157546

Piqueux, S., Edwards, C. S., & Christensen, P. R. (2008). Distribution of the ices exposed near the south pole of Mars using Thermal Emission Imaging System (THEMIS) temperature measurements. *Journal of Geophysical Research*. *113*(E8). https://doi.org/10.1029/2007JE003055

Plaut, J. J., Picardi, G., Safaeinili, A., Ivanov, A. B., Milkovich, S. M., Cicchetti, A., et al. (2007). Subsurface radar sounding of the south polar layered deposits of Mars. *Science*, *316*, 92–95. https://doi.org/10.1126/science.1139672

Plesa, A.-C., Padovan, S., Tosi, N., Breuer, D., Grott, M., Wieczorek, M. A., et al. (2018). The Thermal State and Interior Structure of Mars. *Geophysical Research Letters*, *45*(22), 12198–12209. https://doi.org/10.1029/2018gl080728

Putzig, N. E., Phillips, R. J., Campbell, B. A., Holt, J. W., Plaut, J. J., Carter, L. M., et al. (2009). Subsurface structure of Planum Boreum from Mars Reconnaissance Orbiter Shallow Radar soundings. *Icarus*, *204*, 443–457. https://doi.org/10.1016/j.icarus.2009.07.034

Rutishauser, A., Blankenship, D. D., Sharp, M., Skidmore, M. L., Greenbaum, J. S., Grima, C., et al. (2018). Discovery of a hypersaline subglacial lake complex beneath Devon Ice Cap, Canadian Arctic. *Science Advances*. *4*(4), eaar4353. https://doi.org/10.1126/sciadv.aar4353

Schumacher, S., & Breuer, D. (2006). Influence of a variable thermal conductivity on the thermochemical evolution of Mars. *Journal of Geophysical Research*, *111*(E2). https://doi.org/10.1029/2005JE002429

Selvans, M. M., Plaut, J. J., Aharonson, O., & Safaeinili, A. (2010). Internal structure of Planum Boreum, from Mars advanced radar for subsurface and ionospheric sounding data. *Journal of Geophysical Research*, *115*(E9). https://doi.org/10.1029/2009JE003537

Sori, M. M., & Bramson, A. M. (2019). Water on Mars, with a grain of salt: local heat anomalies are required for basal melting of ice at the south pole today. *Geophysical Research Letters*, *46*(3), 1222–1231. https://doi.org/10.1029/2018GL080985

Spohn, T. (1991). Mantle differentiation and thermal evolution of Mars, Mercury, and Venus. *Icarus*, *90*(2), 222–236. https://doi.org/10.1016/0019-1035(91)90103-Z

Stevenson, D. J. (2007). Earth formation and evolution. *Treatise on Geophysics*, *9*, 1–11. https://doi.org/10.1016/B978-044452748-6.00138-3

Tanaka, K. L., Rodriguez, J. A. P., Skinner, J. A., Bourke, M. C., Fortezzo, C. M., Herkenhoff, K. E., et al. (2008). North polar region of Mars: Advances in stratigraphy, structure, and erosional modification. *Icarus*, *196*, 318–358. https://doi.org/10.1016/j.icarus.2008.01.021

Taylor, G. J., Boynton, W., Brückner, J., Wänke, H., Dreibus, G., Kerry, K., et al. (2006). Bulk composition and early differentiation of Mars. *Journal of Geophysical Research*, *111*(E3). https://doi.org/10.1029/2005je002645

Toner, J. D., Catling, D. C., & Light, B. (2014). The formation of supercooled brines, viscous liquids, and low-temperature perchlorate glasses in aqueous solutions relevant to Mars. *Icarus*, *233*, 36–47. https://doi.org/10.1016/j.icarus.2014.01.018

Turcotte, D., & Schubert, G. (2014). *Geodynamics*. Cambridge, UK: Cambridge University Press.

Wieczorek, M. A. (2008). Constraints on the composition of the Martian south polar cap from gravity and topography. *Icarus*, *196*, 506–517. https://doi.org/10.1016/j.icarus.2007.10.026

Wilson, E. H., Atreya, S. K., Kaiser, R. I., & Mahaffy, P. R. (2016). Perchlorate formation on Mars through surface radiolysis-initiated atmospheric chemistry: A potential mechanism. *Journal of Geophysical Research*, *121*, 1472–1487.

Zuber, M. T., Solomon, S. C., Phillips, R. J., Smith, D. E., Tyler, G. L., Aharonson, O., et al. (2000). Internal structure and early thermal evolution of Mars from Mars global surveyor topography and gravity. *Science*, *287*, 1788–1793. https://doi.org/10.1126/science.287.5459.1788